

CONSENSUS-BASED LOUD DETECTION FOR TRUE AND FALSE WARHEAD RECOGNITION

Kaili Zhang, Qian He*, Zishu He, and Yimin D. Zhang[†]

EE Department, University of Electronic Science and Technology of China, China

[†] Center for Advanced Communications, Villanova University, USA

ABSTRACT

The micro-motion characteristics of warheads have been utilized to discriminate false warheads from true ones. To obtain accurate dimensional measurements, a multiple-input multiple-output (MIMO) radar is adopted to observe the kinetic information of the warhead. A distributed state space model (SSM) is built and the differences between the true and false warheads are characterized as different system parameters of the SSM. In this paper, we extend the locally optimal unknown direction (LOUD) detector, which has shown its effectiveness for hypothesis testing, to the underlying distributed detection problem, and a novel consensus-based LOUD detector is proposed. The superior detection performance of the proposed detection algorithm in identifying the true and false warheads is verified using simulation results.

Index Terms— Ballistic warhead recognition, micro-motion, state space model, LOUD test, broadcast-based consensus algorithm

1. INTRODUCTION

Ballistic missile defense is a critical task that attracted great attentions from many countries. To break the anti-missile interceptor system, the use of advanced false warheads in the middle course phase is reported [1, 2]. Advanced false warheads have almost identical shape and motion as the true ones, making their discrimination from true ones difficult. Different micro-motion characteristics have been exploited to identify the warheads [3]. In particular, the utilization of a multiple-input multiple-output (MIMO) radar with distributed antennas in observing the kinetic information of the warhead enables data collection of the multi-dimensional warhead motion states from multiple distinct directions [4, 5, 6]. Therefore, as compared with traditional radars, the MIMO radar is advantageous in distinguishing the micro-motion characteristics between the true and false warheads.

To directly utilize the available multi-dimensional observation by MIMO radar, a discrete-time state space model (SSM), which includes the micro-motion characteristics, is established to describe the kinetic states of the warhead. As we will show, the difference of micro-motion characteristics between the true and false warheads can be reflected in the parameter matrix of the SSM. For this hypothesis testing, it is shown in [7] that the LOUD detector offers desirable performance in detecting small differences with a small processing

delay [8, 9]. In this paper, we propose a distributed detection algorithm, which is developed under the parallel configuration without fusion center [10], based on the LOUD test and broadcast-based consensus.

In networks of agents, *consensus* means to reach an agreement regarding a certain quantity of interest that depends on the states of all agents [11]. Consensus problems have been widely studied in various fields, including distributed detection [12] and communication [13]. In the broadcast-based consensus algorithm, at every step, one subblock will be randomly chosen to broadcast its state estimates. Subblocks whose distance is within the transmission range will update their state estimates, while the state estimates of the other subblocks will remain unchanged. At the end of the broadcast-update process, one subblock is chosen to make a decision by the LOUD detector according to the updated state estimations. The experimental results show the effectiveness of the proposed method via the comparison with the centralized processing and the distributed detection algorithm with hard-decision processing, both being based on the LOUD detector.

The rest of this paper is organized as follows. The SSM of the warhead flying in the middle course phase and the hypothesis testing for warhead recognition are presented in Section 2. The consensus-based distributed detection method is addressed in Section 3. Simulation results are given in Section 4. Finally, Section 5 provides some concluding remarks.

We use lower-case (upper-case) bold characters to denote vectors (matrices). Throughout this paper, \mathbf{I}_d represents the $d \times d$ identity matrix, $\mathbf{0}_d$ denotes the $d \times d$ matrix with all entries equal to 0, and $\mathbf{1}_d$ stands for a d -dimensional all-one column vector. The symbol $(\cdot)^\dagger$ denotes transpose, and $|\cdot|$ stands for the set cardinality. In addition, $\mathbb{R}^{N \times K}$ represents the complete set of $N \times K$ real matrices. $x \sim \mathcal{N}(a, b)$ implies that the random variable x follows a Gaussian distribution with mean a and variance b .

2. SYSTEM MODEL

2.1. State Equation

Consider the scenario where a warhead is flying in the middle course phase. The compound motion of warhead can be decomposed into translation and micro-motion [14]. Refer to the motion model shown in Fig. 1. We mainly focus on the movement of the dominating scatterer Q , which undergoes both translation and micro-motion. To explicitly analyze the micro-motion of the main scatterer, a reference coordinate system XYZ centered at the intersection of the geometric symmetry axis and the precession axis of the target, initially located at (x_0, y_0, z_0) in UVW , is employed. Assume that the reference coordinate system, parallel to the radar coordinate system, has the same translation as the warhead. The warhead, initially located at

*Correspondence: qianhe@uestc.edu.cn

The work of K. Zhang, Q. He, and Z. He was supported by the National Nature Science Foundation of China under Grants No. 61102142, 61032010, and 61371184, the International Science and Technology Cooperation and Exchange Research Program of Sichuan Province under Grant No. 2013HH0006, and the Fundamental Research Funds for the Central Universities under Grant No. ZYGX2013J015.

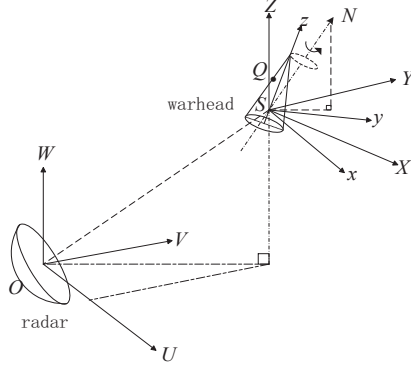


Fig. 1. Warhead movement in radar UVW and reference XYZ coordinate systems.

(x_0, y_0, z_0) , flies with initial translational velocity $(v_{x,0}, v_{y,0}, v_{z,0})$ and acceleration (g_x, g_y, g_z) in UVW . Let $[q_x(t), q_y(t), q_z(t)]$ and $[q'_x(t), q'_y(t), q'_z(t)]$ denote the instantaneous micro-motion position and velocity of Q at time t in XYZ . The instantaneous position $[x(t), y(t), z(t)]$ and the instantaneous velocity $[v_x(t), v_y(t), v_z(t)]$ of Q at time t in UVW can be described by the kinetic equation as follows [14][15]

$$\begin{cases} x(t) = x_0 + v_{x,0}t + 0.5g_x t^2 + q_x(t), \\ y(t) = y_0 + v_{y,0}t + 0.5g_y t^2 + q_y(t), \\ z(t) = z_0 + v_{z,0}t + 0.5g_z t^2 + q_z(t), \\ v_x(t) = v_{x,0} + g_x t + q'_x(t), \\ v_y(t) = v_{y,0} + g_y t + q'_y(t), \\ v_z(t) = v_{z,0} + g_z t + q'_z(t). \end{cases} \quad (1)$$

Define a state vector which contains the instantaneous position, velocity and micro-motion position of the warhead

$$\mathbf{x}(t) = [x(t), y(t), z(t), v_x(t), v_y(t), v_z(t), q_x(t), q_y(t), q_z(t)]^\dagger. \quad (2)$$

According to [7], the continuous-time state equation that describes the dynamic movement, including the micro-motion behaviors, of the warhead can be expressed as

$$\mathbf{x}'(t) = \mathbf{R}_t \mathbf{x}(t) + \mathbf{u}(t), \quad (3)$$

where $\mathbf{x}'(t) = \partial \mathbf{x}(t) / \partial t$ and \mathbf{R}_t is the state transition matrix determined by the micro-motion characteristics of the warhead [7]. Denote the sampling interval by T ($T > 0$), $\mathbf{u}_k = \mathbf{u}(kT)$ and $\mathbf{x}_k = \mathbf{x}(kT)$, the noisy discrete-time state equation can be given by

$$\mathbf{x}_{k+1} = \mathbf{F}_{k+1} \mathbf{x}_k + \mathbf{G}_{k+1} \mathbf{u}_k + \mathbf{w}_{k+1} \quad (4)$$

where

$$\mathbf{F}_{k+1} = e^{\mathbf{R}_t T}, \quad (5)$$

$$\mathbf{G}_{k+1} = \int_0^T e^{\mathbf{R}_t \tau} d\tau. \quad (6)$$

In addition, $\mathbf{u}_k = [0, 0, 0, g_x, g_y, g_z, 0, 0, 0]^\dagger$ denotes the input control vector, and \mathbf{w}_{k+1} is the additive noise vector which is assumed to be white Gaussian with zero mean and covariance matrix Σ_w , i.e., $\mathbf{w}_{k+1} \sim \mathcal{N}(\mathbf{0}, \Sigma_w)$.

2.2. Distributed Observation Equation

Assume that N receive antennas are divided into G subblocks. Subblock g has N_g receive antennas, $g = 1, \dots, G$. Let $s_m(t)$, $m = 1, \dots, M$, denote the transmitted signals, which have normalized energy and are mutually orthogonal. At time k the received signal vector at subblock g is denoted as $\mathbf{r}_k^g(t) = [r_{k1}^g(t), r_{k2}^g(t), \dots, r_{kn_g}^g(t), \dots, r_{kN_g}^g(t)]^\dagger$, where $r_{kn_g}^g(t)$ represents echo accumulated at antenna n_g of subblock g due to the transmissions from the M transmit antennas. Assume at time k , the separated signal model for the mn_g th path at receive antenna n_g of subblock g is

$$r_{kmn_g}^g(t) = \sqrt{E_{km}} \alpha_{kmn_g}^g s_m(t - \tau_{kmn_g}^g) e^{j2\pi f_{kmn_g}^g t} + v_{kmn_g}^g(t), \quad (7)$$

where E_{km} is the m th waveform's transmitted power at time k . The reflection coefficient $\alpha_{kmn_g}^g$, modeled as a zero-mean complex Gaussian random variable, is assumed different for different path and independent of others. In addition, $v_{kmn_g}^g(t)$ represents zero-mean, complex Gaussian noise, spatially and temporally white with autocorrelation function $\sigma_v^2 \delta(\tau)$. $\tau_{kmn_g}^g$ and $J_{kmn_g}^g$ represent the time delay and Doppler shift, respectively.

With the echoes processed at subblock g , a noise corrupted model of the warhead state values, \mathbf{x}_k , is generated using a maximum likelihood (ML) estimator [16]. It can be expressed as

$$\mathbf{z}_k^g = \mathbf{H} \mathbf{x}_k + \mathbf{e}_k^g, \quad g = 1, \dots, G, \quad (8)$$

where \mathbf{H} is referred to as the system observation matrix, and $\mathbf{e}_k^g \sim \mathcal{N}(\mathbf{0}, \Sigma_e^g)$.

Thus, the SSM of the warhead composes of the state equation (4) and the distributed observation equation (8). The true and false warheads mainly differ in the parameter matrix \mathbf{F}_{k+1} of the SSM, which is utilized to complete warhead target recognition [7].

2.3. Hypothesis Testing

In the initial stage, the true and false warheads have the same motion state values, i.e., $\mathbf{F}_{k+1} = \mathbf{F}_0$. Due to the separation of the true and false warheads at time n , \mathbf{F}_{k+1} become different. On account of self-controller, the true warhead keeps in a steady state, i.e., $\mathbf{F}_{k+1} = \mathbf{F}_0$. The false warhead, on the other hand, has different micro-motions, such as tumbling and swing, leading to a different unknown transition matrix $\mathbf{F}_{k+1} = \mathbf{F}_c$. As such, it renders an abrupt change detection problem [17], which can be solved via a binary hypothesis testing method.

We take each receive subblock as a detection unit. Then, the local hypothesis testing at subblock g is built as follows

$$H_0 : \mathbf{z}_k^g, \quad k = 0, 1, \dots, n, \\ \mathbf{F}_{k+1} = \begin{cases} \mathbf{F}_0, & k = 0, 1, \dots, n-2, \\ \mathbf{F}_0, & k = n-1, \end{cases} \quad (9)$$

$$H_1 : \mathbf{z}_k^g, \quad k = 0, 1, \dots, n, \\ \mathbf{F}_{k+1} = \begin{cases} \mathbf{F}_0, & k = 0, 1, \dots, n-2, \\ \mathbf{F}_c, & k = n-1. \end{cases}$$

3. CONSENSUS-BASED DISTRIBUTED DETECTION

3.1. Broadcast-Based Consensus

We treat G subblocks as the nodes of an undirected and connected graph $\mathcal{G} = (\mathcal{V}, \mathcal{E})$, where \mathcal{V} is the set of vertices with $|\mathcal{V}| = G$,

and \mathcal{E} is the set of edges. The edge formation is related to node communication connectivity, i.e., each pair of nodes is connected if their Euclidean distance is smaller than transmission radius d named connectivity radius. We assume that a communication within this transmission radius always succeeds. Note that this model is a simple graph. The neighbors of subblock g are denoted by $\mathcal{A}(g) = \{h \in \mathcal{V} : (g, h) \in \mathcal{E}\}$.

Here, we use an asynchronous time model which has been employed in [18] and [19]. In this model, we assume that each subblock is equipped with a local clock. Each clock of a subblock ticks independently according to a Poisson process with rate λ . Essentially, this is equivalent to a single clock which ticks according to a Poisson process with rate $G\lambda$. Clearly, the probability that one particular subblock's clock ticks at a given time is equal to the probability that any other clock ticks, which is equal to $1/G$. We use the number of clock ticks $\{0, 1, 2, \dots, n_k\}$ as a measure of time, where n_k represents the time when the last broadcast occurs during the k th observation interval $[kT, (k+1)T]$. Next, we will consider the broadcast-update process during the k th observation interval $[kT, (k+1)T]$.

Suppose subblock g 's clock ticks at the beginning of the $(n+1)$ th time slot. Subblock g then broadcasts its state values to all its neighboring subblocks. The group states will be updated as follows

$$\mathbf{z}_k^h(n+1) = \begin{cases} \mathbf{z}_k^h(n) + \gamma[\mathbf{z}_k^{g,h}(n) - \mathbf{z}_k^h(n)], & h \in \mathcal{A}(g), \\ \mathbf{z}_k^h(n), & h \notin \mathcal{A}(g), \end{cases} \quad (10a)$$

where $\gamma \in (0, 1)$ is usually referred to as the mixing parameter. In the above expression, $\mathbf{z}_k^{g,h}(n) = \mathbf{z}_k^g(n) + \mathbf{v}_k^{g,h}(n)$, where $\mathbf{v}_k^{g,h}(n)$ represents stochastic perturbation and its elements are independent random variables with zero-mean and a finite variance. Then, the state updating equation (10a) can be expanded as

$$\mathbf{z}_k^h(n+1) = (1-\gamma)\mathbf{z}_k^h(n) + \gamma\mathbf{z}_k^g(n) + \gamma\mathbf{v}_k^{g,h}(n), \quad h \in \mathcal{A}(g). \quad (11)$$

Using the matrix notations, $\mathbf{Z}_k(n) = [\mathbf{z}_k^1(n), \dots, \mathbf{z}_k^G(n)]^\dagger$ and $\mathbf{V}_k(n) = [\mathbf{v}_k^1(n), \dots, \mathbf{v}_k^G(n)]^\dagger$, where $\mathbf{v}_k^h(n)$ is an $L \times 1$ column vector, defined by

$$\mathbf{v}_k^h(n) = \begin{cases} \mathbf{0}, & h \notin \mathcal{A}(g), \\ \gamma\mathbf{v}_k^{g,h}(n), & h \in \mathcal{A}(g). \end{cases} \quad (12)$$

We can combine (10b) and (11) into a compact form as

$$\mathbf{Z}_k(n+1) = \mathbf{P}(n)\mathbf{Z}_k(n) + \mathbf{V}_k(n), \quad (13)$$

where $\mathbf{P}(n) \in \mathbb{R}^{G \times G}$ is a stochastic matrix, which, with probability $1/G$ and assuming subblock g 's clock ticks, takes the following value

$$\mathbf{P}(n) = \mathbf{I} - \gamma \sum_{h \in \mathcal{A}(g)} (\varepsilon_h \varepsilon_h^\dagger - \varepsilon_h \varepsilon_g^\dagger), \quad (14)$$

where ε_h represents a column vector with the h th element to be 1 and the rest to be 0. It is easy to verify that $\mathbf{P}(n)\mathbf{1} = \mathbf{1}$.

Note that similar to the analysis in [18], we can prove that the broadcast-based consensus algorithm will converge to a consensus almost surely, in the absence of the perturbation vector $\mathbf{V}_k(n)$.

3.2. LOUD-Based Test Statistics

During the k th observation interval $[kT, (k+1)T]$, the observation vector will be updated to $\mathbf{z}_k^g(n_k)$. For the LOUD detector [7], the

test statistics at subblock g can be expressed as

$$\Gamma_{\text{LOUD}}^g(\mathbf{z}_{k+1}^g(n_{k+1})) = \frac{\sum_{j=1}^{L'} \sum_{i=1}^{L'} \frac{\partial^2 p(\mathbf{z}_{k+1}^g(n_{k+1}) | \mathbf{z}_k^g(n_k); \mathbf{F}_{k+1})}{\partial \mathbf{F}_{k+1}^2(i, j)}}{p(\mathbf{z}_{k+1}^g(n_{k+1}) | \mathbf{z}_k^g(n_k); \mathbf{F}_0)} \Bigg|_{\mathbf{F}_{k+1} = \mathbf{F}_0}, \quad (15)$$

where L' is the dimension of the square matrix \mathbf{F}_{k+1} . Note in (8) that \mathbf{H} is an $L \times L'$ matrix. As usually $L < L'$, \mathbf{H} is singular. In this case, we consider Kalman filter iterations to calculate the test statistics.

Combining (8) and (13), we are led to

$$\mathbf{z}_k^g(n_k) = \mathbf{H}\mathbf{x}_k + \tilde{\mathbf{e}}_k^g, \quad g = 1, \dots, G. \quad (16)$$

The detailed description of $\tilde{\mathbf{e}}_k^g$ is omitted here due to space limitation.

Equations (4) and (16) form the SSM of the warhead for the consensus-based distributed detection. In the following, we derive the test statistics of the consensus-based distributed LOUD detector.

First, we define $\mathcal{Z}_k^g \triangleq \{\mathbf{z}_0^g(n_0), \mathbf{z}_1^g(n_1), \dots, \mathbf{z}_k^g(n_k)\}$. Combining the consensus-based SSM and Kalman filter method, the definitions of $\mathbf{x}_{k|k}$, $\Sigma_{k|k}^{\mathbf{x}}$, $\mathbf{z}_{k|k}^g$ and $\Sigma_{k|k}^g$ can be obtained. Then present the iteration process and are expressed as

$$\begin{aligned} \mathbf{x}_{k|k} &= \mathbf{x}_{k|k-1} + \Sigma_{k|k-1}^{\mathbf{x}} \mathbf{H}^\dagger \left(\mathbf{H} \Sigma_{k|k-1}^{\mathbf{x}} \mathbf{H}^\dagger + \Sigma_{\tilde{\mathbf{e}}}^g \right)^{-1} \\ &\quad \times \left(\mathbf{z}_k^g(n_k) - \mathbf{H} \mathbf{x}_{k|k-1} \right), \end{aligned} \quad (17)$$

$$\begin{aligned} \Sigma_{k|k}^{\mathbf{x}} &= \Sigma_{k|k-1}^{\mathbf{x}} - \Sigma_{k|k-1}^{\mathbf{x}} \mathbf{H}^\dagger \left(\mathbf{H} \Sigma_{k|k-1}^{\mathbf{x}} \mathbf{H}^\dagger + \Sigma_{\tilde{\mathbf{e}}}^g \right)^{-1} \\ &\quad \times \mathbf{H} \Sigma_{k|k-1}^{\mathbf{x}}, \end{aligned} \quad (18)$$

$$\mathbf{x}_{k+1|k} = \mathbf{F}_{k+1} \mathbf{x}_{k|k} + \mathbf{G}_{k+1} \mathbf{u}_k, \quad (19)$$

$$\Sigma_{k+1|k}^{\mathbf{x}} = \mathbf{F}_{k+1} \Sigma_{k|k}^{\mathbf{x}} \mathbf{F}_{k+1}^\dagger + \Sigma_{\mathbf{w}}, \quad (20)$$

$$\mathbf{z}_{k+1|k}^g = \mathbf{H} \mathbf{x}_{k+1|k}, \quad (21)$$

$$\Sigma_{k+1|k}^g = \mathbf{H} \Sigma_{k|k}^{\mathbf{x}} \mathbf{H}^\dagger + \Sigma_{\tilde{\mathbf{e}}}^g. \quad (22)$$

We can conclude as follows

$$\mathbf{z}_{k+1}^g(n_{k+1}) | \mathcal{Z}_k^g \sim \mathcal{N} \left(\mathbf{z}_{k+1|k}^g, \Sigma_{k+1|k}^g \right). \quad (23)$$

Then, $p(\mathbf{z}_{k+1}^g(n_{k+1}) | \mathcal{Z}_k^g; \mathbf{F}_0)$ can be obtained.

Next we define

$$\begin{aligned} \Pi_{k+1}^g(i, j) &= \frac{\partial^2 p(\mathbf{z}_{k+1}^g(n_{k+1}) | \mathcal{Z}_k^g; \mathbf{F}_{k+1})}{\partial \mathbf{F}_{k+1}^2(i, j)} \Bigg|_{\mathbf{F}_{k+1} = \mathbf{F}_0} \\ &= \frac{1}{(\Delta F)^2} \left[p(\mathbf{z}_{k+1}^g(n_{k+1}) | \mathcal{Z}_k^g; \mathbf{F}_0(i, j) + \Delta F) \right. \\ &\quad \left. + p(\mathbf{z}_{k+1}^g(n_{k+1}) | \mathcal{Z}_k^g; \mathbf{F}_0(i, j) - \Delta F) \right. \\ &\quad \left. - 2p(\mathbf{z}_{k+1}^g(n_{k+1}) | \mathcal{Z}_k^g; \mathbf{F}_0(i, j)) \right]. \end{aligned} \quad (24)$$

The LOUD-based test statistics in (15) can be calculated as

$$\Gamma_{\text{LOUD}}^g(\mathbf{z}_{k+1}^g(n_{k+1})) = \frac{\sum_{j=1}^{L'} \sum_{i=1}^{L'} \Pi_{k+1}^g(i, j)}{p(\mathbf{z}_{k+1}^g(n_{k+1}) | \mathcal{Z}_k^g; \mathbf{F}_0)}. \quad (25)$$

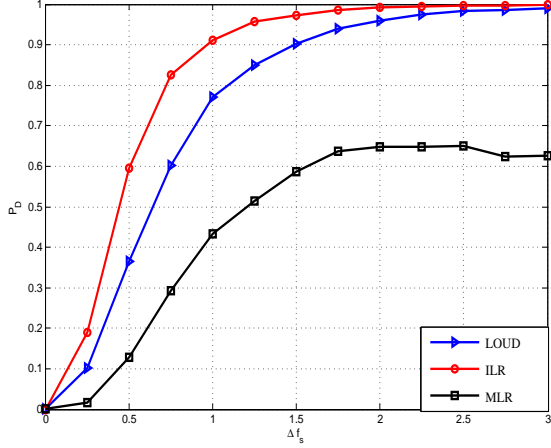


Fig. 2. P_D of LOUD, ILR, and MLR detectors based on consensus algorithm versus the Δf_s .

4. NUMERICAL RESULTS

Consider a MIMO radar equipped with $M = 4$ transmit antennas and $N = 8$ receive antennas. The receive array is divided into three subblocks. The total transmit energy is $E = 25$. Consider the spinning motion of the warhead. The \mathbf{F}_{k+1} in (4) has the form as follows

$$\mathbf{F}_{k+1} = \begin{bmatrix} \mathbf{I}_3 & T\mathbf{I}_3 & \frac{1}{2}(T\omega_s\Omega_s)^2 \\ \mathbf{0}_3 & \mathbf{I}_3 & T\omega_s^2\Omega_s^2 + \frac{1}{2}T^2\omega_s^3\Omega_s^3 \\ \mathbf{0}_3 & \mathbf{0}_3 & \mathbf{I}_3 + T\omega_s\Omega_s + \frac{1}{2}T^2\omega_s^2\Omega_s^2 \end{bmatrix},$$

which is dependent on the rotation angular frequency $\omega_s = 2\pi f_s$ with the initial rotation frequency $f_s = 1\text{Hz}$ and

$$\Omega_s = \begin{bmatrix} 0 & -\omega_z & \omega_y \\ \omega_z & 0 & -\omega_x \\ -\omega_y & \omega_x & 0 \end{bmatrix}$$

where the micro-motion vector $[\omega_x, \omega_y, \omega_z] = [0.6, 0.5, 0.6245]$. Set the sampling time interval $T = 0.1$ s. Further, the acceleration vector is assumed to be $\mathbf{u}_k = [0, 0, 0, 0, 2, 9.6, 0, 0]^\dagger$, the initial state vector as $\mathbf{x}_0 = [100, 200, 1000, 100, 50, 10, 0.05, 0.06, 0.08]^\dagger$ and the covariance matrix of the state noise as $\Sigma_w = 0.2\mathbf{I}_9$. We define Δf_s as the rotation frequency change of the false warhead, which characterizes the difference of the micro-motion between the true and false warheads.

Denote $\mathbf{H} = [\mathbf{I}_6, \mathbf{0}_{6 \times 3}]$. Assume that the lowpass equivalents of the transmitted waveforms are frequency spread single Gaussian pulse signals, expressed as

$$s_k(t) = \left(\frac{2}{T_t}\right)^{\frac{1}{4}} \exp\left(\frac{-\pi t^2}{T_t^2}\right) \exp(j2\pi k\Delta f t), \quad (26)$$

where $T_t = 0.1$ and $\Delta f = 0.7/T_t$ are used to guarantee the orthogonality. Assume Σ_e^g to be a diagonal matrix with diagonal elements determined by the Cramer-Rao bound (CRB) for the estimates of the warhead's position and velocity [6].

To evaluate the effectiveness of the consensus-based distributed LOUD detector, Fig. 2 shows the detection probability P_D of LOUD, ideal likelihood ratio (ILR), and mismatched likelihood ratio (MLR) detectors [7] versus the Δf_s . Under the assumptions that two arbitrary subblocks are within the transmission range of each other

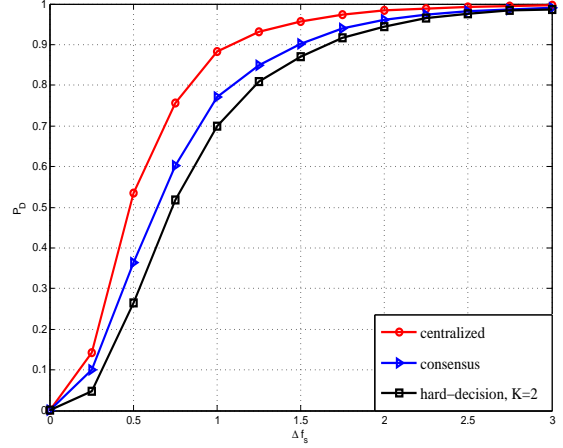


Fig. 3. P_D of centralized, consensus, and hard-decision distributed algorithms based on LOUD detector versus the Δf_s .

and no additive stochastic perturbations, it is easy to verify that this algorithm converges to a consensus almost surely. In this figure, the probability of false alarm P_F is set to be 10^{-3} and the mixing parameter is chosen to be $\gamma = 0.5$. Note that, for LOUD-based detectors, the test statistic is computed from (24) and (25), whereas for the ILR and MLR, it is directly obtained because of the assumed known \mathbf{F}_c . The P_D result is shown with respect to Δf_s for $\Delta f_s \in [0, 3]$. It is clear from Fig. 2 that the LOUD detector achieves a higher P_D than the MLR detector, performs similarly to the ILR detector and achieves unit P_D when Δf_s reaches 3. As such, the results evidently demonstrate the effectiveness of the proposed method in computing the LOUD-based test statistics.

Fig. 3 compared the detection performance of the consensus-based LOUD detector with the centralized LOUD detector and the hard-decision distributed method. The parameter setting of the consensus-based distributed LOUD detector in Fig. 3 is the same as that in Fig. 2. The hard-decision distributed LOUD detector makes a global decision according to K/G criterion at fusion center with $K = 2$. Compared to the centralized detection algorithm, the proposed distributed detection algorithm significantly reduces the required communication load and the achieved detection probability is slightly inferior. On the other hand, the proposed algorithm outperforms the hard-decision method in the studied case. Therefore, the proposed method is considered as an attractive approach when low data transmission is desirable.

5. CONCLUSION

Based on MIMO radar observations, an SSM is built to describe the kinetic motion of the warhead. The difference in micro-motion characteristics between the true and false warheads can be reflected as the difference of the SSM parameters. Ballistic warhead recognition is then turned into a binary hypothesis test problem. We propose a newly distributed detection algorithm, which contains the broadcast-based consensus algorithm and LOUD test. In the case that the observation matrix is singular, we adopt Kalman filter iterations to obtain the LOUD-based test statistics. Finally, simulation results demonstrate that the proposed algorithm achieves a high identification accuracy, which is close to ideal centralized processor under particular conditions.

6. REFERENCES

- [1] W. Z. Lemnios and A. A. Grometstein, "Overview of the Lincoln Laboratory ballistic missile defense program," *Lincoln Laboratory Journal*, vol. 13, no. 1, pp. 9–32, 2002.
- [2] X. R. Li and V. P. Jilkov, "Survey of maneuvering target tracking. Part II: Motion models of ballistic and space targets," *IEEE Transactions on Aerospace and Electronic Systems*, vol. 46, no. 1, pp. 96–119, 2010.
- [3] V. C. Chen, F. Li, S-S. Ho, and H. Wechsler, "Analysis of micro-Doppler signatures," *IEE Proceedings-Radar, Sonar and Navigation*, vol. 150, no. 4, pp. 271–276, 2003.
- [4] A. M. Haimovich, R. Blum S, and L. J. Cimini, "MIMO radar with widely separated antennas," *IEEE Signal Processing Magazine*, vol. 25, no. 1, pp. 116–129, 2008.
- [5] E. Fishler, A. Haimovich, R. S. Blum, L. J. Cimini, D. Chizhik, and R. A. Valenzuela, "Spatial diversity in radars—Models and detection performance," *IEEE Transactions on Signal Processing*, vol. 54, no. 3, pp. 823–838, 2006.
- [6] Q. He, R. S. Blum, and A. M. Haimovich, "Noncoherent MIMO radar for location and velocity estimation: More antennas means better performance," *IEEE Transactions on Signal Processing*, vol. 58, no. 7, pp. 3661–3680, 2010.
- [7] X. Wang, Q. He, and D. Cai, "Sequential LOUD test for genuine and dummy warhead identification using MIMO radar," in *Proceedings of International Conference on Communications, Signal Processing, and Systems (CSPS)*. Huhehaote, China, July 2014.
- [8] Q. He and R. S. Blum, "Smart grid monitoring for intrusion and fault detection with new locally optimum testing procedures," in *Proceedings of IEEE International Conference on Acoustics, Speech and Signal Processing (ICASSP)*, 2011, pp. 3852–3855.
- [9] Q. He and R. S. Blum, "New hypothesis testing-based rapid change detection for power grid system monitoring," *International Journal of Parallel, Emergent and Distributed Systems*, vol. 29, no. 3, pp. 239–263, 2013.
- [10] R. Viswanathan and P. K. Varshney, "Distributed detection with multiple sensors. I. Fundamentals," *Proceedings of the IEEE*, vol. 85, no. 1, pp. 54–63, 1997.
- [11] R. Olfati-Saber, J. A. Fax, and R. M. Murray, "Consensus and cooperation in networked multi-agent systems," *Proceedings of the IEEE*, vol. 95, no. 1, pp. 215–233, 2007.
- [12] R. Olfati-Saber, E. Franco, E. Frazzoli, and J. S. Shamma, "Belief consensus and distributed hypothesis testing in sensor networks," in *Networked Embedded Sensing and Control*, pp. 169–182. Springer, 2006.
- [13] Z. Li, F. R. Yu, and M. Huang, "A distributed consensus-based cooperative spectrum-sensing scheme in cognitive radios," *IEEE Transactions on Vehicular Technology*, vol. 59, no. 1, pp. 383–393, 2010.
- [14] A. Farina, B. Ristic, and D. Benvenuti, "Tracking a ballistic target: Comparison of several nonlinear filters," *IEEE Transactions on Aerospace and Electronic Systems*, vol. 38, no. 3, pp. 854–867, 2002.
- [15] R. K. Mehra, "A comparison of several nonlinear filters for reentry vehicle tracking," *IEEE Transactions on Automatic Control*, vol. 16, no. 4, pp. 307–319, 1971.
- [16] H. V. Poor, *An Introduction to Signal Detection and Estimation*, Springer, 1994.
- [17] M. Basseville and I. V. Nikiforov, *Detection of Abrupt Changes: Theory and Application*, vol. 104, Prentice Hall, 1993.
- [18] Y. Yang and R. S. Blum, "Broadcast-based consensus with non-zero-mean stochastic perturbations," *IEEE Transactions on Information Theory*, vol. 59, no. 6, pp. 3971–3989, 2013.
- [19] T. C. Aysal, M. E. Yildiz, A. D. Sarwate, and A. Scaglione, "Broadcast gossip algorithms for consensus," *IEEE Transactions on Signal Processing*, vol. 57, no. 7, pp. 2748–2761, 2009.